Paper:

Development of Mobile Robot System Equipped with Camera and Laser Range Finder Realizing HOG-Based Person Following and Autonomous Returning

Masashi Awai*, Atsushi Yamashita, Takahito Shimizu*, Toru Kaneko*, Yuichi Kobayashi*, and Hajime Asama****

*Department of Mechanical Engineering, Shizuoka University
3-5-1 Johoku, Naka-ku, Hamamatsu-shi, Shizuoka 432-8561, Japan
E-mail: tykobay@ipc.shizuoka.ac.jp
**Department of Precision Engineering, The University of Tokyo
7-3-1 Hongo, Bunkyo-ku, Tokyo 113-8656, Japan
[Received September 10, 2013; accepted November 7, 2013]

In this paper, we propose a mobile robot system which has functions of person following and autonomous returning. The robot realizes these functions by analyzing information obtained with camera and laser range finder. Person following is performed by using HOG features, color information, and pattern of range data. Along with person following, a map of the ambient environment is generated from range data. Autonomous returning to the starting point is performed by applying potential method to the generated map. We verified the proposed method by experiment using a wheel mobile robot in an indoor environment.

Keywords: mobile robot, laser range finder, camera, person following

1. Introduction

In recent years, introduction of autonomous mobile robots to environments close to us is expected. Examples include shopping cart robots returning automatically to the shopping cart shed after shopping and guide robots directing the way from the current location to the starting point in unknown environments. A robot that accomplishes these purposes needs functions of person following and autonomously returning to the starting point [1–3].

In reference [1] and reference [2], returning was performed after arrival at the destination by manual control. However, manual control of the robot requires great care. In reference [3], person following and autonomous returning were performed. However, autonomous returning was performed only by tracing the route recorded on the outward way.

We previously proposed in reference [4] a mobile robot system which has functions of person following and autonomous returning to the starting point while avoiding obstacles. In this system, person following was performed by detection of moving object using Laser Range Finder (LRF) and person extraction using color information. However, detection of moving object was unstable depending on the walking speed. Therefore, We need more stable person following method.

Person following methods were proposed in references [5–7]. A method in reference [5] detected persons by template matching of legs-like pattern for LRF data. To follow the target person, it employed particle filtering whose initial particles were generated from infrared image. A method in reference [6] used stereo camera and detected persons by depth templates of person shape. It employed the Extended Kalman filter for person following. A method in reference [7] used LRF and omni-view camera. LRF data were used for detecting candidate of person regions and omni-view camera images were used for extracting person regions based on HOG (Histogram of Oriented Gradients) features. It also employed particle filtering for person following.

The abovementioned methods for person following used one or two criteria for person detection. Here, note that addition of criterion for person detection increases the robustness of person following if one criterion itself works well.

Therefore, in this paper we propose a mobile robot which has a function of robust person following realized by integration of three criteria for person detection based on pattern of LRF data, HOG features and color histogram. The robot also has a function of self localization for map generation on the outward way, and a function of autonomous return with obstacle avoidance.

2. Outline

In this paper, we verify the system using a mobile robot equipped with a Laser Range Finder (LRF) and a camera (**Fig. 1**). The mobile robot acquires two dimensional (2-D) range data of 180° forward by the LRF. The mobile robot also acquires the image in the front direction by the camera.

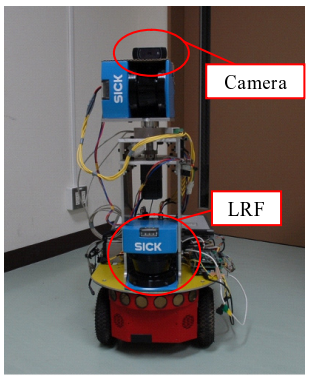

Fig. 1. Mobile robot.

Fig. 2. Environment.

The mobile robot detects and follows a person by using the LRF and the camera when moving on the outward way. At the same time, the mobile robot generates a map with range data measured by the LRF.

The mobile robot generates a potential field from the generated map by an artificial potential method. Then, it moves on the return way along gradient directions of the generated potential field. At the same time, the mobile robot avoids obstacles not recorded in the map by reconstruction of the potential field.

An operating environment of the mobile robot is a flat floor where the mobile robot moves in 2-D space (**Fig. 2**). In the operating environment, multiple objects and pedestrians usually exist. In this situation, person following by a single method of person detection may be difficult. It will be realized by combining multiple methods of person detection.

3. Person Following on Outward Way

The mobile robot performs person following and map generation on the outward way. In this paper, the mobile robot follows the person by using person detection.

Person detection is performed by evaluating a value of person likelihood. The value of person likelihood can be evaluated on the pattern of range data and the HOG features in acquired images. However, this evaluation is ineffective to follow the person in environment where more than one person exist. The reason for this is that the pattern of LRF data and HOG features are not specific to the person who should be followed but common to all persons. Under an assumption that pedestrians do not wear clothes with similar color to the person to be followed, color information is added to the pattern of range data and HOG features. Thus, person following is performed by using particle filter based on pattern of range data, HOG features and color information.

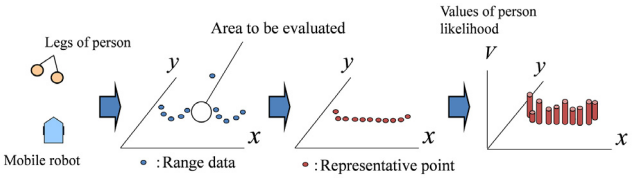

Fig. 3. Points of data evaluation.

3.1. Tracking by Particle Filter

We use a particle filter [8] for person following. The particle filter estimates the position of the person to be followed on a horizontal plane. In this study, density of particle distribution represents the probability of existence of the person to be followed. By calculating particle positions according to the particle filter algorithm, position of the person to be followed can be estimated.

In particle filter algorithm, a particle is assigned a weight at each particle position. However, calculation of weight at each particle position is computationally expensive. Thus, assigning the weight to the particle is performed at representative points. Representative points are set at the positions of range data basically. But here we have to notice that points in between legs are not evaluated through the process. Therefore, process to cover points in between legs should be performed. **Fig. 3** shows process of determining representative points.

First, the robot acquires range data. Distance $D(\theta)$ and angle θ are obtained as the range data in polar coordinates. Initially, representative points $\vec{R} = (U(\theta)\cos(\theta), U(\theta)\sin(\theta))$ are set using the range data as $U(\theta) = D(\theta)$. Process to cover points in between legs is performed by Eq. (1), which will be applied to each range data.

$$U(\theta) = \min_{-k<l<k} D(\theta+l) \quad \text{if } (D(\theta+l+k) < D(\theta+l)), \quad \ldots\ldots \quad (1)$$

$$k = \arctan\left(\frac{W}{2D(\theta+l)}\right), \quad \ldots\ldots\ldots \quad (2)$$

where W is estimated value of length in between legs.

Next, values of person likelihood are evaluated at each representative position. In the particle filter algorithm, particles near to representative points are assigned a weight as evaluated values $V(\vec{R})$. Thus, calculating $V(\vec{R})$ is performed only at representative points close to particles.

Particle filter is performed as follows.

(i) Initial particles are distributed around the person with random noise.

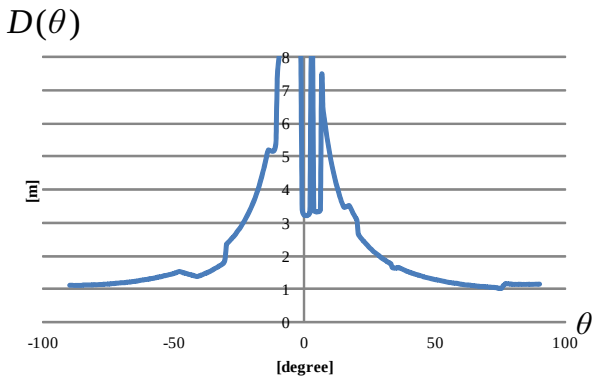

Fig. 4. Range data.

(ii) Particles are moved based on the system model given by Eq. (3).

$$\vec{x}_{t|t-1} = \vec{x}_{t-1} + \vec{v}_{t-1}T, \quad \ldots\ldots\ldots \quad (3)$$

where $\vec{x}_t$ is an estimated position vector of the person on a horizontal plane at time t, $\vec{v}_t$ is velocity vector of the person at time t, and T is time of updating cycle. $\vec{v}_t$ is estimated by the subtraction of $\vec{x}_{t-1}$ and $\vec{x}_{t-2}$.

(iii) Each particle is assigned a weight w as following equation.

$$w = \frac{V(\mathbf{R}) \exp\left(-\frac{D^2}{2\sigma}\right)}{\sqrt{2\pi\sigma}}, \quad \ldots\ldots\ldots \quad (4)$$

where σ is position error. Position error includes error of self-location estimation and measuring error. However, these error are hard to define. Thus, position error is defined as the constant value empirically. D is distance between the particle and the nearest range data, $V(\mathbf{R})$ is value of likelihood of the nearest representative point.

(iv) Estimated position $\vec{x}_t$ is determined by calculating center of gravity of particles. Position $\vec{x}_t$ is regarded as the position of the person to be followed at time t. Thus, the mobile robot move toward the position $\vec{x}_t$ at time t.

(v) New particles are selected in descending order according to the weight as resampling process.

First, process (i) is performed. Next, processes (ii), (iii) and (iv) are performed. After that, processes (ii), (iii), (iv) and (v) are performed repeatedly.

3.2. Evaluation on Pattern of Range Data

Person detection is performed by using pattern of range data. Range data is acquired as shown in **Fig. 4** in the environment (**Fig. 5**). In the reference [5], person following was performed by template matching from LRF data. In the study, person following was achieved by using templates with 7 position-relation patterns of person

Fig. 5. Acquired image.

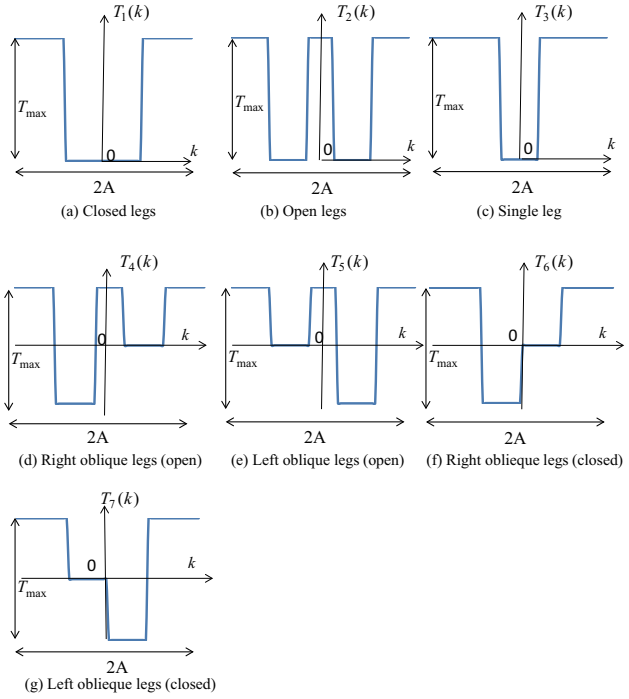

Fig. 6. Leg templates.

legs. Therefore, as the evaluation on pattern of range data, pattern matching is performed by using range data and 7 templates of legs that are the same as [5] in our study. The 7 patterns are shown in **Fig. 6**, where relative position of legs are varied as closed, open, left forward, right forward and so on.

While following the person, matching scores are obtained by performing pattern matching at all representative positions $\vec{R}(\theta, U(\theta))$. Matching score $L(\vec{R})$ is obtained at each $\vec{R}$ by Eq. (5):

$$L(\vec{R}) = 2AT_{max} - S(\vec{R}), \quad \ldots\ldots\ldots \quad (5)$$

$$S(\vec{R}) = \min_{1 \le i \le N} \sum_{k=-A}^{A} |(D(\theta+k) - U(\theta)) - T_i(k)|, \quad (6)$$

$$A = \arctan\left(\frac{W}{2U(\theta)}\right), \quad \ldots\ldots\ldots \quad (7)$$

where N is number of template, A is width of templates, T_{max} is the value set to a maximum value of $((D(\theta+k) - U(\theta)))$.

Fig. 7. Dataset.

3.3. Evaluation on HOG Features

Person detection in acquired images is performed by using Real AdaBoost algorithm [9] with HOG features. The validity of HOG features for person detection is verified in the reference [10].

Thus, classifier of Real AdaBoost for person detection is generated from HOG features of sample images of person and background. Daimler Pedestrian Classification Benchmark Dataset [a] is used as sample images (**Fig. 7**).

Real AdaBoost constructs the strong classifier as linear combination of weak classifier.

$$H = \sum_{d=1}^{D} h_d, \quad \ldots \ldots \ldots \ldots \ldots \quad (8)$$

where D is the number of weak classifier, H is value of strong classifier, h_d is value of weak classifier. We use value of H as the constructed strong classifier value of Real AdaBoost.

For person detection on HOG features, image regions to perform person detection are selected in acquired images. $H(\vec{R})$ is acquired at each representative point $\vec{R}$. By setting the size of person, size and position of the image region are determined according to each representative point $\vec{R}$.

3.4. Evaluation on Color Histogram

Detecting the person who should be followed is performed by using color histogram. The color histogram of hue h and saturation s is made (an example of hue-saturation histogram is depicted in **Fig. 8** with an image of a person in an indoor environment). Number of bins of hue $\times$ saturation set to 16×8. This setting is based on experiment with human identification conducted by Takahashi et al. [11], where histogram of $h = 16 \times s = 8$ was verified to be effective to make identification robust to the changes of brightness.

The mobile robot acquires color information on the person to be followed by the mobile robot before the person following begins.

While the mobile robot follows the person, the color information is acquired from the image region which is selected according to each position of representative point. Assuming that the ordinary size of person and the distance between camera and person are known, image regions can be determined according to the representative point $\vec{R}$. Then, the color histogram is made and the similarity with the color histogram made before the person following begins is calculated.

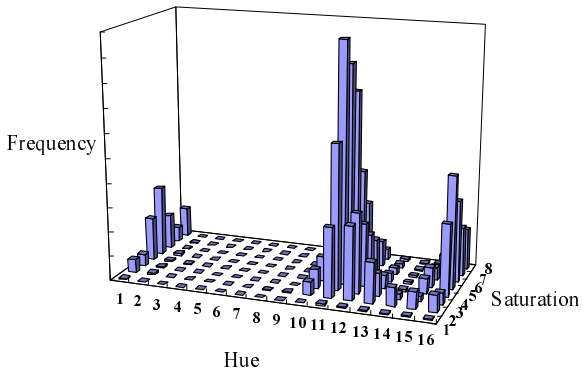

Fig. 8. An example of color histogram.

The Bhattacharyya coefficient [12] is used for calculating the similarity with the histograms. Eq. (9) shows Bhattacharyya coefficient $C(\vec{R})$ of point $\vec{R}$.

$$C(\vec{R}) = \sum_{h=0}^{h_b} \sum_{s=0}^{s_b} \sqrt{H_t(h,s) \times H(h,s,\vec{R})}, \quad \ldots \quad (9)$$

where $H_t(h,s)$ is the frequency of each bin of the color histogram of the person that is acquired before the mobile robot begins person following. $H(h,s,\vec{R})$ is the frequency of each bins of the color histogram acquired in image region for position $\vec{R}$ while the mobile robot follows the person. h_b is the number of bins of hue h, and s_b is the number of bins of saturation s.

3.5. Integration of Evaluated Values by PCA

The integrated value of person likelihood $V(\vec{R})$ is calculated by applying PCA (Principal Component Analysis) to $L(\vec{R})$, $H(\vec{R})$ and $C(\vec{R})$. Before PCA is performed, averaging procedure is performed. This procedure is introduced because large differences of values among representative points in the near distance can be noise for PCA. Averaged values $L_s(\vec{R}), H_s(\vec{R}), C_s(\vec{R})$ are calculated by following equations.

$$L_s(\vec{R}_i) = \sum_{j}^{a_i} L(\vec{R}_j), \quad \ldots \ldots \ldots \ldots \quad (10)$$

$$H_s(\vec{R}_i) = \sum_{j}^{a_i} H(\vec{R}_j), \quad \ldots \ldots \ldots \ldots \quad (11)$$

$$C_s(\vec{R}_i) = \sum_{j}^{a_i} C(\vec{R}_j), \quad \ldots \ldots \ldots \ldots \quad (12)$$

where $\vec{R}_j$ is representative point having the distance between $\vec{R}_i$ and $\vec{R}_j$ not more than threshold d_a, a_i is number of $\vec{R}_j$.

Next, for processing PCA, standardized value ($V_L(\mathbf{R})$, $V_H(\mathbf{R})$, $V_C(\mathbf{R})$) is calculated from $L_s(\vec{R})$, $H_s(\vec{R})$ and $C_s(\vec{R})$

as the followings.

$$V_L(\vec{R}) = \frac{L_s(\vec{R}) - \overline{L_s(\vec{R})}}{s_L}, \quad \ldots\ldots\ldots \quad (13)$$

$$V_H(\vec{R}) = \frac{H_s(\vec{R}) - \overline{H_s(\vec{R})}}{s_H}, \quad \ldots\ldots\ldots \quad (14)$$

$$V_C(\vec{R}) = \frac{C_s(\vec{R}) - \overline{C_s(\vec{R})}}{s_C}, \quad \ldots\ldots\ldots \quad (15)$$

where $\overline{L(\vec{R})}, \overline{H(\vec{R})}, \overline{C(\vec{R})}$ are averages, s_L, s_H, s_C are variances. PCA is processed by calculating eigenvector from variance-covariance matrix $\sum$ from $V_L(\vec{R})$, $V_H(\vec{R})$, $V_C(\vec{R})$.

$$\sum = \begin{pmatrix} S(V_L,V_L) & S(V_L,V_H) & S(V_L,V_C) \\ S(V_H,V_L) & S(V_H,V_H) & S(V_H,V_C) \\ S(V_C,V_L) & S(V_C,V_H) & S(V_C,V_C) \end{pmatrix}, \quad (16)$$

where $S(V_i,V_j)$ is covariance of V_i and V_j.

Finally, the integrated value of person likelihood $V(\vec{R})$ is calculated by using the primary ingredient (α,β,γ) and eigenvalue of the primary ingredient λ.

$$V(\vec{R}) = \alpha V_L(\vec{R}) + \beta V_H(\vec{R}) + \gamma V_C(\vec{R}) + 2\sqrt{\lambda}. \quad (17)$$

To avoid negative effect by a large noise, a coefficient is set zero when its corresponding component has negative value.

4. Map Generation on Outward Way

The mobile robot generates the map of ambient environment while it moves on the outward way. The LRF is used to measure the ambient environment during the mobile robot movement, and the ambient environment map is generated by integrating each measurement data. Measurement data integration needs an accurate self-location estimation of the mobile robot. In this study, the estimation is made by dead reckoning. However, dead reckoning has a problem of error accumulation caused by wheel slipping. In order to decrease this error accumulation, the robot aligns each measurement data by the ICP algorithm [13].

Moving objects do not exist in the same place. Therefore, it is necessary to remove moving objects from the map. The mobile robot removes moving objects by a method in the reference [14]. To remove a moving object, subtraction of acquired range data at different robot positions is performed. The map of static object can be acquired by using this method.

5. Motion on Return Way

The mobile robot moves on the return way according to the Laplace potential method [15]. The robot generates the potential field in the map obtained on the outward way.

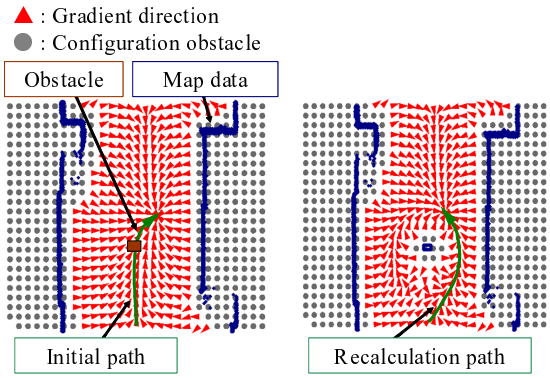

(a) Initial path. (b) Recalculation path.

Fig. 9. Reconstruction of potential field.

Then the robot moves on the return way along a gradient direction of the generated potential field.

For the robot to avoid obstacles not recorded in the map, the LRF measures an ambient environment while the robot moves on the return way and the robot reconstructs a potential field. **Fig. 9** shows reconstruction of a potential field. If the robot detects an obstacle which did not exist on the outward way, the obstacle is added to the map data made on the outward way (**Fig. 9(a)**). Then the robot reconstructs a potential field to avoid obstacles (**Fig. 9(b)**). This makes the movement of the robot safe on the return way.

6. Experiment

6.1. Experimental Device

We used the mobile robot "Pioneer 3" of MobileRobots, Inc. (**Fig. 2**). The robot has 2 drive wheels and 1 caster. It's maximum speed is 400 mm/sec. It turns with the velocity differential of right and left wheels. The LRF is model LMS200-30106 by SICK. It is equipped at a height of 300 mm above the ground. The sensing range is 180° in one plane and the resolution is 0.5°. The camera is model C910 by logicool. Its horizontal angle of view is about 70°. The camera is equipped at a height of 800 mm above the ground. As the specs on computers, CPU is Intel Core 2Duo T9300 2.5 GHz, and memory is 3.5 GB.

6.2. Experiment Environment

We conducted experiment in which the mobile robot follows a person to the target point and then returns to the starting point. Experiment environment was a corridor with a flat floor. **Fig. 2** shows the experiment environment.

The width of corridor is about 2 m. Wall materials are metal and concrete. There were two pedestrians on vinyl flooring in experiment environment. We set position error $\sigma = 50$ mm, parameter of LRF detection $T_{max} = 700$ mm, parameters of color histogram $h_b = 16$, $s_b = 8$, and parameter $d_a = 50$ mm.

Fig. 10. Acquired image (A).

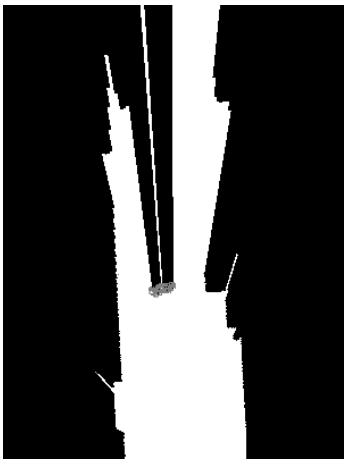

Fig. 11. 2-D map image (A).

Fig. 12. Particles in 2-D map image (A).

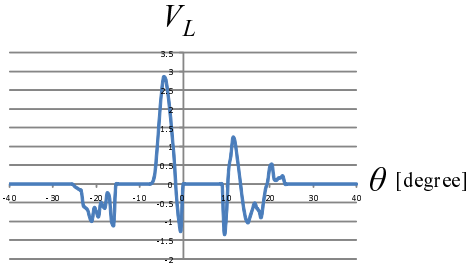

Fig. 13. Evaluation value of LRF $V_L(\theta)$ (A).

Fig. 14. Person detection by HOG features (A).

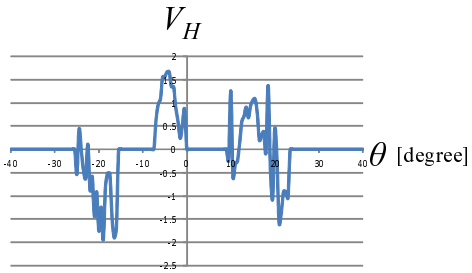

Fig. 15. Evaluation value of HOG $V_H(\theta)$ (A).

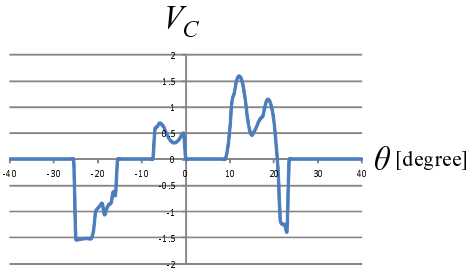

Fig. 16. Evaluation value of color histogram $V_C(\theta)$ (A).

6.3. Experimental Result

On the outward way, the mobile robot followed the person. **Fig. 10** shows an image acquired with the camera while the robot followed the person.

Figure 11 shows particles and a 2-D map image generated by range data acquired with the LRF. Gray points in 2-D map are particles. **Fig. 12** shows the magnified map around particles in **Fig. 11**.

Figure 13 shows evaluation value on shape of range data $V_L(\theta)$. The horizontal axis in **Fig. 13** indicates the view angle from the robot (the positive and negative values correspond to the right and left angle, respectively). In **Fig. 13**, it is shown that high values appear in the vicinity of the angle where the person exists.

Figure 14 shows person detection by HOG features. **Fig. 15** shows evaluation value on HOG features $V_H(\theta)$. In **Fig. 14**, white rectangles are the regions whose value of $V_H(\theta)$ exceeded the threshold. It is shown that high values appear in the vicinity of the angle where the person exists.

Figure 16 shows evaluation value on color information $V_C(\theta)$. The obstacle which has the similar color to the person to be followed was existing in the right side of the person. It is shown that high values appear in the vicinity of the angle where the obstacle exists (vicinity of 13°).

Finally, **Fig. 17** shows the integrated value of person likelihood $V(\theta)$. It is shown that the highest values appear in the vicinity of the angle where the person to be followed exists.

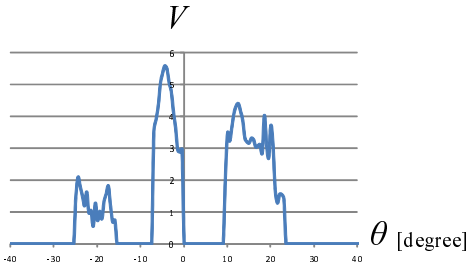

Fig. 17. Integrated evaluation value $V(\theta)$ (A).

Fig. 18. Acquired image (B).

Fig. 19. 2-D map image (B).

Fig. 20. Particles in 2-D map image (B).

Figure 18 shows an image acquired with the camera while the pedestrian passed. In **Fig. 18**, the right person is to be followed by the mobile robot. **Figs. 19** and **20** show particles and a 2-D map image. **Fig. 21** shows $V_L(\theta)$. **Fig. 22** shows person detection by HOG features. **Fig. 23** shows $V_H(\theta)$. **Fig. 24** shows $V_C(\theta)$. **Fig. 25** shows $V(\theta)$.

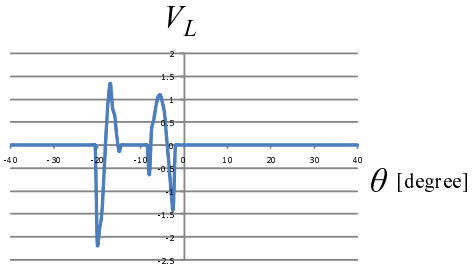

Fig. 21. Evaluation value of LRF $V_L(\theta)$ (B).

Fig. 22. Person detection by HOG features (B).

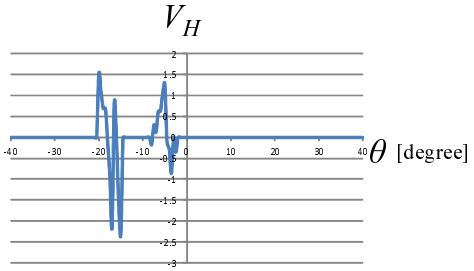

Fig. 23. Evaluation value of HOG $V_H(\theta)$ (B).

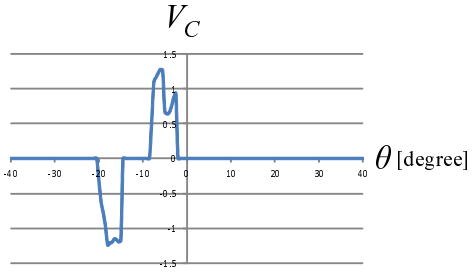

Fig. 24. Evaluation value of color histogram $V_C(\theta)$ (B).

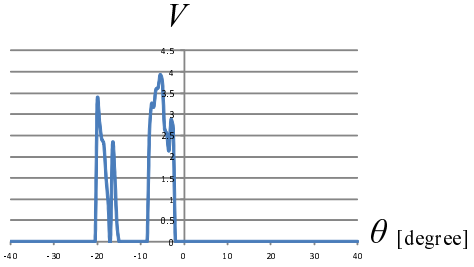

Fig. 25. Integrated evaluation value $V(\theta)$ (B).

Table 1. Ratio of frame whose person's point has highest value.

	k LRF (V_L)	HOG (V_H)	Color (V_C)	Integrated (V)
Number of frame	236	209	228	242
Rate of frame [%]	95.5	84.6	92.3	97.9

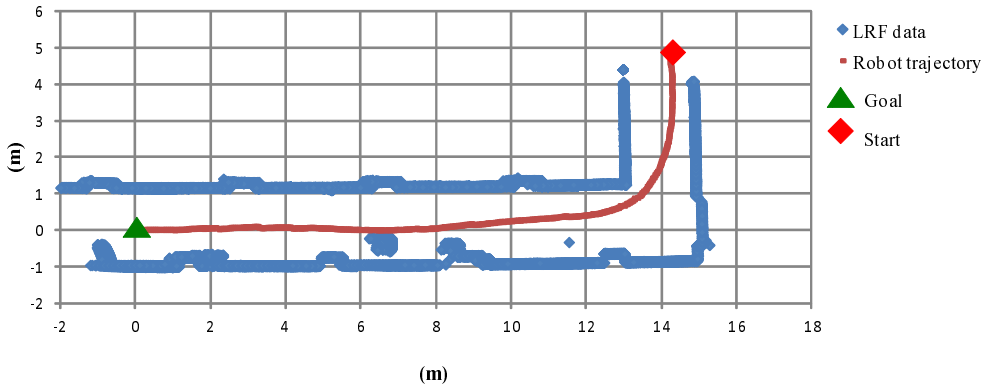

Fig. 26. Generated map and trajectory of mobile robot on the outward way.

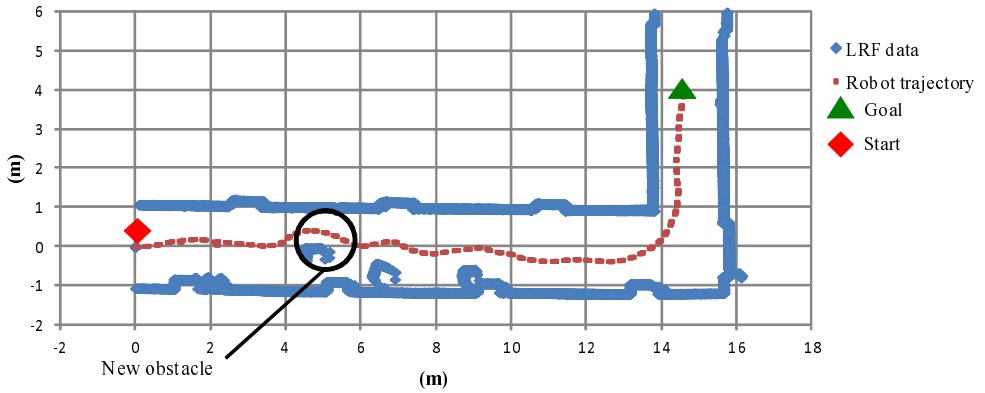

Fig. 27. Generated map and trajectory of mobile robot on the return way.

In **Figs. 21** and **23**, it is shown that high values appear in the vicinity of the angle where the person exist (vicinities of 5° and 20°). In **Fig. 24**, it is shown that high values appear only in the vicinity of the angle where the person to be followed exists.

Finally, in **Fig. 25**, it is shown that the highest values appear in the vicinity of the angle where the right person to be followed exists. Thus, it is more effective to use integrated value than to use LRF value or HOG value.

The number of acquired images and range data during person following was 349 frame. The number of frames containing objects outside the person to be followed was 247 frame.

Table 1 shows ratio of the frame which the highest value appears where the person to be followed exists among frames containing objects outside the person to be followed. It is shown that integrated value has the highest ratio.

Figure 26 shows the generated map and the robot trajectory on the outward way. It is shown that stationary object map was generated by moving object detection.

Figure 27 shows the trajectory of the robot on the return way. The robot moved on the return way by using the map which had been generated on the outward way. On the return way, the obstacle that did not exist on the outward way appeared. It is shown that the robot returned to the starting position while avoiding the obstacle.

These results show that the mobile robot can detect and follow the person by the proposed method in the experimental environment and can return to the starting point while avoiding obstacles.

The error between the starting point in **Fig. 26** and the goal point in **Fig. 27** may be caused by error of ICP method. The reason for this is that features along the moving direction in **Figs. 26** and **27** for alignment of ICP method were sparse in experimental environment.

7. Conclusion

In this paper, we constructed the mobile robot system that has functions of person following and returning to the starting location autonomously while avoiding obstacles.

Person following was achieved by using pattern of range data, HOG features and color information. Map generation was achieved by the ICP algorithm and the moving object detection. The robot returned to the starting point according to the Laplace potential method with generated map and a path of avoiding obstacle is generated by reconstructing a potential field.

As future works, we need to conduct experiments in more diverse situations (many people, longer distance). This requires functions of supporting occlusion and more precise localization in dynamic environment. Furthermore, in the situation that pedestrians wearing same color clothes exist, the proposed method may not be effective. In such cases, utilization of time-series information will play more important role. More precise and robust system model in the particle filter (or other filter techniques) will be required.

Acknowledgements

This work was in partly supported by the Kayamori Foundation of Informational Science Advancement, and MEXT KAKENHI, Grantin-Aid for Young Scientist (A), 22680017.

References:

[1] M. Misawa, T. Yoshida, and S. Yuta, "A Smart Handcart with Autonomous Returning Function," J. of Robotics Society of Japan, Vol.25, No.8, pp. 1199-1206, 2007 (in Japanese).

[2] T. Lixin and S. Yuta, "Mobile Robot Playback Navigation Based on Robot Pose Calculation Using Memorized Omnidirectional Images," J. of Robotics and Mechatronics, Vol.14, No.4, pp. 366-374, 2002.

[3] N. Tsuda, S. Harimoto, T. Saitoh, and R. Konishi, "Mobile Robot with Following and Returning Mode," Proc. of the 18th IEEE Int. Symposium on Robot and Human Interactive Communication (RO-MAN2009), ThB1.3, pp. 933-938, 2009.

[4] T. Shimizu, M. Awai, A. Yamashita, and T. Kaneko, "Mobile Robot System Realizing Human Following and Autonomous Returning Using Laser Range Finder and Camera," Proc. of the 18th Korea-Japan Joint Workshop on Frontiers of Computer Vision (FCV2012), 2012.

[5] S. Okusako and S. Sakane, "Human Tracking with a Mobile Robot using a Laser Range-Finder," J. of Robotics Society of Japan, Vol.24, No.5, pp. 605-613, 2006 (in Japanese).

[6] J. Satake and J. Miura, "Person Following of a Mobile Robot using Stereo Vision," J. of Robotics Society of Japan, Vol.28, No.9, pp. 1091-1099, 2010 (in Japanese).

[7] M. Saito, K. Yamazaki, N. Hatao, R. Hanai, K. Okada, and M. Inaba, "Pedestrian Detection using a LRF and a Small Omni-view Camera for Outdoor Personal Mobility Robot," Proc. of the 2010 IEEE Int. Conf. on Robotics and Biomimetics (ROBIO 2010), pp. 196-201, 2010.

[8] M. Isard and A. Blake, "Condensation-conditional density propagation for visual tracking," Int. J. of Computer Vision, Vol.29, No.1, pp. 5-28, 1998.

[9] R. E. Schapire and Y. Singer, "Improved boosting algorithms using confidence rated predictions," Machine Learning, No.37, pp. 297-336, 1999.

[10] N. Dalal and B. Triggs, "Histograms of Oriented Gradients for Human Detection," Proc. of the 2005 IEEE Computer Society Conf. on Computer Vision and Pattern Recognition (CVPR2005), pp. 886-893, 2005.

[11] H. Takahashi, K. Nakamura, H. Zhao, and R. Shibasaki, "Human Identification Using Laser Scanners and Image Sensors," Proc. of Asian Conf. on Remote Sensing 2007, TS24-2, 2007.

[12] T. Kailath, "The Divergence and Bhattacharyya Distance Measures in Signal Selection," IEEE Trans. on Communication Technology, Vol.COM-15, No.1, pp. 52-60, 1967.

[13] P. J. Besl and N. D. Mckay, "A Method for Registration of 3-D Shapes," IEEE Trans. on Pattern Analysis and Machine Intelligence, Vol.14, No.2, pp. 239-256, 1992.

[14] S. Iwashina, A. Yamashita, and T. Kaneko, "3-D Map Building in Dynamic Environments by a Mobile Robot Equipped with Two Laser Range Finders," Proc. of the 3rd Asia Int. Symposium on Mechatronics, TP1-3(1), pp. 1-5, 2008.

[15] K. Sato, "Deadlock-free Motion Planning Using the Laplace Potential Field," Proc. of the Joint Int. Conf. on Mathematical Methods and Supercomputing in Nuclear Applications, pp. 449-461, 1994.

Supporting Online Materials:

[a] Daimler Pedestrian Classification Benchmark Dataset, http://www.gavrila.net/Datasets/datasets.html

Name:
Masashi Awai

Affiliation:
Ctec, Inc.

Address:
35th Floor, Mori Tower, Roppongi Hills, 6-10-1 Roppongi, Minato-ku, Tokyo, Japan

Brief Biographical History:

2013 Received Master degree from Graduate School of Engineering, Shizuoka University
2013- Ctec, Inc.

Name:
Atsushi Yamashita

Affiliation:
Associate Professor, Department of Precision Engineering, The University of Tokyo

Address:
7-3-1 Hongo, Bunkyo-ku, Tokyo 113-8656, Japan

Brief Biographical History:

2001-2008 Assistant Professor, Shizuoka University
2006-2007 Visiting Associate, California Institute of Technology
2008-2011 Associate Professor, Shizuoka University
2011- Associate Professor, The University of Tokyo

Main Works:

• "Motion Planning of Multiple Mobile Robots for Cooperative Manipulation and Transportation," IEEE Trans. on Robotics and Automation, Vol.19, No.2, pp. 223-237, Apr. 2003.
• "Parallel Line-based Structure from Motion by Using Omnidirectional Camera in Texture-less Scene," Advanced Robotics, Vol.27, No.1, pp. 19-32, Jan. 2013.

Membership in Academic Societies:

• The Institute of Electrical and Electronics Engineers (IEEE)
• Association for Computing Machinery (ACM)
• The Robotics Society of Japan (RSJ)
• The Japan Society of Mechanical Engineers (JSME)
• The Japan Society for Precision Engineering (JSPE)
• The Institute of Electronics, Information and Communication Engineers (IEICE)
• The Institute of Electrical Engineers of Japan (IEEJ)
• Information Processing Society of Japan (IPSJ)
• The Institute of Image Information and Television Engineers (ITE)
• The Society of Instrument and Control Engineers (SICE)
• Society for Serviceology

Name:
Takahito Shimizu

Affiliation:
Iwata Shinkin Bank

Address:
578-1 Nakaizumi, Iwata-shi, Shizuoka, Japan

Brief Biographical History:
2012 Received Master degree from Graduate School of Engineering, Shizuoka University
2012- Iwata Shinkin Bank

Name:
Toru Kaneko

Affiliation:
Professor, Graduate School of Engineering, Shizuoka University

Address:
3-5-1 Johoku, Naka-ku, Hamamatsu-shi, Shizuoka, Japan

Brief Biographical History:
1974- Nippon Telegraph and Telephone Corporation
1987- NTT Human Interface Laboratories
1997- Faculty of Engineering, Shizuoka University

Main Works:
• "Chroma Key Using a Checker Pattern Background," IEICE Trans. on Information and Systems, Vol.90-D, No.1, pp. 242-249, Jan. 2007.

Membership in Academic Societies:
• The Institute of Electrical and Electronics Engineers (IEEE)
• The Institute of Electronics, Information and Communication Engineers (IEICE)
• The Institute of Image Information and Television Engineers (ITE)

Name:
Yuichi Kobayashi

Affiliation:
Associate Professor, Graduate School of Engineering, Shizuoka University

Address:
3-5-1 Johoku, Naka-ku, Hamamatsu-shi, Shizuoka, Japan

Brief Biographical History:
2002- Research Scientist, RIKEN Bio-mimetic Control Research Center
2007- Associate Professor, Tokyo University of Agriculture and Technology
2012- Associate Professor, Shizuoka University

Main Works:
• "Planning-Space Shift Motion Generation: Variable-space Motion Planning Toward Flexible Extension of Body Schema," J. of Intelligent and Robotic Systems, Vol.62, Issue 3-4, Jun. 2011.

Membership in Academic Societies:
• The Institute of Electrical and Electronics Engineers (IEEE)
• The Robotics Society of Japan (RSJ)
• The Society of Instrument and Control Engineers (SICE)
• The Japan Society of Mechanical Engineers (JSME)
• The Japan Society for Precision Engineering (JSPE)

Name:
Hajime Asama

Affiliation:
Professor, Department of Precision Engineering, The University of Tokyo

Address:
7-3-1 Hongo, Bunkyo-ku, Tokyo 113-8656, Japan

Brief Biographical History:
1986- Research Associate, RIKEN (The Institute of Physical and Chemical Research)
1998- Professor, RACE (Research into Artifacts, Center for Engineering), The University of Tokyo
2002- Professor, Department of Precision Engineering, School of Engineering, The University of Tokyo

Main Works:
• "Adaptive Division-of-Labor Control Algorithm for Multi-robot Systems," J. of Robotics & Mechatronics, Vol.22, No.4, pp. 514-525, Aug. 2010.

Membership in Academic Societies:
• The Institute of Electrical and Electronics Engineers (IEEE)
• The Robotics Society of Japan (RSJ)
• The Japan Society of Mechanical Engineers (JSME)
• The Japanese Society of Instrumentation and Control Engineers (SICE)